Instability-Driven Branching of Lamellar Crystals in Polyethylene Spherulites

Akihiko Toda,* Ken Taguchi, and Hiroshi Kajioka

Graduate School of Integrated Arts and Sciences, Hiroshima University, 1-7-1 Kagamiyama, Higashi-Hiroshima 739-8521, Japan

Received May 2, 2008; Revised Manuscript Received August 11, 2008

ABSTRACT: The mechanism of instability-driven branching of lamellar crystallites in the formation of polymer spherulites has been examined experimentally for polyethylene-banded spherulites in terms of the molecular weight dependence by optical and atomic force microscopies associated with quenching and chemical etching. The possibility of instability-driven branching has been suggested by the experimental results of our previous work in terms of the temperature dependences of the band spacing, the lamellar width at the growth front, and the growth rate. The examination of the dependences on the average and distribution of molecular weights enables us to differentiate possible origins of the instability, e.g., compositional gradient with the diffusion of uncrystallized fractions and pressure gradient caused by the density difference between the crystal and the melt. The experimental results suggest the instability driven by the pressure gradient in the melt ahead of the growth front.

1. Introduction

Spherulite is a basic higher-order structure of crystalline polymers, and the formation is a general phenomenon when crystallized from the melt. Polymer spherulite evolves with radiating and space-filling branches of chain-folded lamellar crystallites by means of consecutive branching and reorientation of lamellae. The mechanism of branching and reorientation is therefore the most important issue to be clarified in the formation mechanism. In our previous papers,[1−3] we have proposed a mechanism by incorporating the instability-driven branching of individual crystals and their spontaneous reorientation with inherent surface stresses.

In terms of the reorientation of lamellar crystals in the spherulites, there are two possibilities of the higher order structures, i.e., banded and nonbanded spherulites. In the banded spherulites, a concentric ring pattern appears as the result of twisting reorientation of lamellae along the radial direction, as has been clarified by polarizing optical microscopy (POM)[4−7] and microbeam X-ray diffraction.[8,9] For the evolution of the ring pattern in banded spherulites, twisting reorientation is therefore the necessary condition. The loss of twisting reorientation results in the formation of nonbanded spherulites. In this type of nonbanded spherulites without twisting reorientation, a patchy pattern is recognized instead of the concentric rings and indicates a random reorientation, which has been confirmed by the combination of an image analysis of POM[3] and microbeam X-ray diffraction.[10] For the reorientation of lamellar crystals, it has been supposed that the chain folding and ciliation on the folding surfaces will be the origin of the intrinsic and unbalanced surface stresses.[11,12]

On the basis of those evidence and suggestions of reorientation of lamellar crystals in the spherulites, in our previous papers,[1−3] we have examined banded spherulites of polyethylene (PE) and poly(vinylidene fluoride) (PVDF) and nonbanded spherulites of poly(butene-1) (PB-1). The structure of those spherulites and the morphology of lamellar crystals at the growth front have been examined by POM, atomic force microscopy (AFM), and transmission electron microscopy. It has been confirmed that the maximum width of lamellar crystals at the growth front, λ_m, limits the band spacing, P, in the banded spherulites of PE[1] and PVDF[2] and the persistence length of the patchy pattern, L, in the nonbanded spherulites of PB-1;[3] namely, the proportional relationships between them has been confirmed experimentally as, $P, L \propto \lambda_m$.

It has been further suggested that the maximum lamellar width, λ_m, is determined by the branching mechanism driven by an instability at the growth front of individual crystals. The possibility of the instability of growth front has been discussed for many years since the original proposal by Keith and Padden[13] without firm experimental evidence of the branching at the expected length scale. In our previous paper, by examining the temperature dependence of P, L and λ_m in the banded spherulites of PE and PVDF and the nonbanded spherulites of PB-1, the following dependences have been experimentally confirmed: $P, L \propto \lambda_m \propto (k_T/V)^{1/2}$, where k_T represents the temperature dependence of Vogel−Fulcher type and V is the growth rate of spherulites. The dependence of $V^{-1/2}$ suggested the morphological instability driven by the balance between the enhancement effect due to a gradient in chemical potential ahead of the growth front and the suppression due to surface tension of the crystal−melt interface. On the other hand, the temperature dependence of k_T can be of the diffusion coefficient, D, of polymer molecules or of the viscosity, η. Therefore, the dependence on $(k_T/V)^{1/2}$ has suggested the instability driven by a compositional gradient, as originally suggested by Keith and Padden,[13] or by a pressure gradient inducing the flow to supply the difference in the crystalline and molten densities. Due to the same temperature dependence of D and η^{-1}, the distinction of the origin of the gradient field could not be made in the previous papers.[1−3]

As continuing work on the mechanism of instability-driven branching, in the present paper, we further approach the origin of the gradient field by examining the molecular weight dependence of P and λ_m in PE banded spherulites. We expect the different dependences of D and η on the weight-averaged molecular weight, M_w, and the strong dependence of the compositional gradient on the distribution of molecular weight represented by M_w/M_n. By examining those dependences, we will make the differentiation of the gradient field. In the following, we first review our modeling on the branching and reorientation mechanism in the formation of polymer spherulites. Then, the experimental results with various M_w and M_w/M_n of PE are discussed.

* Corresponding author. Tel: +81-82-424-6558. Fax: +81-82-424-0757. E-mail: atoda@hiroshima-u.ac.jp.

10.1021/ma800994g CCC: $40.75
Published on Web 09/26/2008

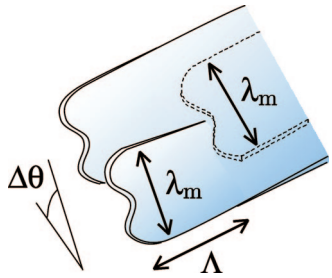

Figure 1. Schematic illustration of the evolution of crystal branching at the critical width, λ_m, and the angle of reorientation, $\Delta\theta$, between the successive branching.

2. Modeling

Branching and Reorientation. As the source of branching and reorientation of lamellar crystals in the morphological evolution of polymer spherulites with space-filling branches, our modeling[1] supposes that the growth front wider than a critical width, λ_m, becomes unstable and splays into a pair of branches. Then, the reorientation due to intrinsic surface stresses results in the independent growth of each branch, which can grow in width as well as in length, so that the width of each branch can become wider than λ_m again. Consequently, the branching will be repeated at the growth front, as schematically shown in Figure 1. The modeling has common features with the morphological observations of the repetitive lamellar twisting and splaying in a banded spherulite confirmed by Briber and Khoury[14] and the branching and splaying of individual dominant lamellae in banded and nonbanded polymer spherulites confirmed by Bassett et al.[15−17]

Concerned with the origin of the surface stresses, it is known that the folding of chains needs larger cross section than crystalline stems,[18] and hence the steric hindrance and the congestion of folds, cilia, and tie chains induce stress on the upper and lower surface regions of thin lamellar crystallites. The stresses are the origin of the lamellar reorientation, which results in the nonplanar conformation of lamellar crystals. Therefore, the origin of reorientation in our modeling is based on the detailed discussions on the unbalanced surface stresses by Lotz and Cheng[11] and on the pressure from cilia confined between lamellae by Bassett and Olley.[16]

In terms of the direction of reorientation, there are two possibilities with and without the twisting correlation of lamellar crystallites along the radial direction of spherulite. Banded spherulites can be formed by the twisting correlation, and the loss of twisting correlation results in the formation of nonbanded spherulites. For banded spherulites, the stress will be torsional and the lamellar crystals twist in the same direction. In our previous paper,[1] we have discussed the relationship between the band spacing, P, and the critical lamellar width, λ_m, and concluded that the higher-order structure is determined by the width of the building blocks; that is the width of lamellar crystals at the growth front, λ_m. The band spacing is in proportion to the lamellar width, λ_m, for both of the cases of nonuniform twist on the occasion of branching and continuous twist limited by lamellar width[19]

$$P = \frac{\pi g}{\Delta\theta}\lambda_m \tag{1}$$

where the coefficient $g/\Delta\theta$ represents the axial ratio of growth rate, g, and the angle of twist between successive branching, $\Delta\theta$.

On the other hand, for nonbanded spherulites, the stress will not be torsional, and the direction of reorientation will be chosen in a random manner depending on the local surface stresses at the growth front. Then, instead of the appearance of periodic banding, the correlation of lamellar orientation along the radial direction will be lost exponentially. For the reorientation of lamellar crystals, the higher-order structure of the patchy pattern is again determined by the width of the building blocks; namely, the persistence length, L, is proportional to the critical width, λ_m, as[3]

$$L = \frac{g}{2\Delta\theta^2}\lambda_m \tag{2}$$

with both of the nonuniform reorientation on the occasion of branching and the continuous reorientation limited by lamellar width.[19]

Instability-Driven Branching. For the determining mechanism of the critical width of lamellar crystals at the growth front of spherulites, our modeling[1] supposes a self-induced gradient field in the melt ahead of the growth front. The gradient can be compositional or pressure, as discussed below. Due to the field, there must be a gradient in the chemical potential of the melt, and hence in the gradient of the difference between the melt and crystal, $\Delta\mu$, expressed as

$$\Delta\mu \simeq \Delta\mu_0 + a(y - y_0) \tag{3}$$

where $\Delta\mu_0$ represents the difference at the interface, $y = y_0$, and $a(>0)$ represents the gradient in the y direction normal to the interface.

The gradient enhances the fluctuations of the growth front because of larger driving force, $\Delta\mu$, at $y > y_0$, while the surface tension of the crystal melt interface, γ, suppresses the fluctuations. The balance of the two effects determines the critical wavelength above which the fluctuations can grow. We suppose that the critical wavelength corresponds to the lamellar width just before branching, i.e., the maximum width at the growth front, λ_m. Then, the maximum width is represented as[1]

$$\lambda_m = 2\pi\left(\frac{v_s\gamma}{a}\right)^{1/2} \tag{4}$$

with the gradient, a, the surface tension, γ, and the specific volume of a segment in the crystal, v_s.

Regarding the instability caused by a gradient field, the most well-known one will be of Mullins−Sekerka's type[20,21] caused by the compositional gradient at the growth front in the liquid side. As the source of compositional gradient, Keith and Padden[13] suggested the noncrystallizing fractions diffusing out from the growth front. Actually, synthetic polymers inevitably have common characteristics of multicomponent systems with molecular weight distribution and defects in the chain structure, both of which introduce the distribution of melting temperatures and hence of chemical potential difference, $\Delta\mu$. On the basis of the chemical potential of Flory−Huggins's type[22] with two (crystallizing and noncrystallizing) components, the maximum width of eq 4 is given as,[1]

$$\lambda_m \simeq 2\pi\left(\frac{x_1 v_s\gamma}{\Delta c k_B T}\frac{D}{V}\right)^{1/2} \tag{5}$$

for the growth front moving at the velocity, V. Here, x_1 represents the number of segments in the polymer chain of noncrystallizing component, Δc the built-up concentration of the noncrystallizing component at the growth front, D the coefficient of interdiffusion, k_B the Boltzmann constant, and T the crystallization temperature. It is noted that the width, λ_m, is not directly proportional to D/V, as has been supposed in the original Keith and Padden's model,[13] but depends on the square root of D/V due to the suppression effect of surface tension, as was suggested by Goldenfeld.[23]

On the other hand, we can also suppose another type of instability driven by the difference in the crystal and liquid

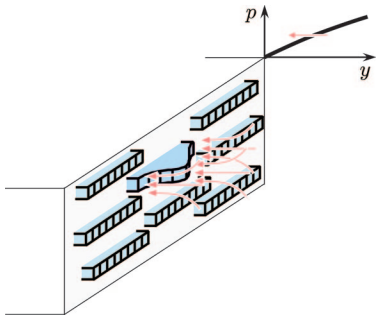

Figure 2. Schematic illustration of pressure gradient spontaneously formed at the growth front of a spherulite and the shear flow induced by the gradient.

densities. Due to the difference, there must be a flow to supply polymer molecules to the growth front, and the flow must be driven by a mechanical (pressure) gradient in the viscous melt (Figure 2); the possibility of the self-induced field of pressure gradient in polymer crystallization has been pointed out by Schultz.[24] The gradient can be the origin of the instability similar to Saffman−Taylor instability[25,26] of so-called "viscous fingering" caused by the pressure gradient in a viscous fluid.

The change in pressure, dp, induces the change in the chemical potential difference, $\Delta\mu$, due to the Clausius−Clapeyron relation of the melting line. Then, the gradient in the chemical potential, a, is determined as

$$a = \frac{\Delta h_f}{T_m}\frac{\partial(\Delta T)}{\partial y} = \frac{\Delta h_f}{T_m}\left(\frac{\Delta v}{\Delta S}\frac{\partial p}{\partial y}\right) = \Delta v\frac{\partial p}{\partial y} \tag{6}$$

where T_m and ΔT represent the melting point and the degree of supercooling, respectively, Δh_f and ΔS represent the heat of fusion and the entropy of melting per segment, respectively, and Δv represents the difference in the specific volume of a segment between the crystal and the melt.

On the other hand, the pressure gradient in the fluid of viscosity, η, induces the shear flow of thickness, b, with the flow rate, u, which balances the density difference, as

$$\frac{\partial p}{\partial y} = \frac{12\eta}{b^2}u = \frac{12\eta}{b^2}\frac{\Delta v}{v_s}V \tag{7}$$

From eqs 4, 6, and 7, the maximum lamellar width is expressed as[1]

$$\lambda_m = 2\pi b\frac{v_s}{\Delta v}\left(\frac{\gamma}{12\eta V}\right)^{1/2} \tag{8}$$

where the factor $\eta V/\gamma$ is the capillary number representing the relative effect of viscous forces versus surface tension.

From the expressions of eqs 1, 5, and 8, the dependence on the growth condition of the ring period, P, and the maximum width, λ_m, is summarized as

$$P \propto \lambda_m \propto \left(\frac{k}{V}\right)^{1/2} \tag{9}$$

with the coefficient k determined by the nature of the gradient field. If the compositional gradient is the case, as was originally suggested by Keith and Padden,[13] k is proportional to the diffusion coefficient of polymers, D. For the case of pressure gradient, k is inversely proportional to the viscosity, η.

In our previous paper,[1,2] the relationship of eq 9 has been examined in terms of the temperature dependence for the growth of PE and PVDF banded spherulites. Owing to Einstein's relation, the temperature dependence of k in eq 9 is identical for the compositional gradient (D) and for the pressure gradient (η^{-1}) in the temperature range high enough from the glass transition temperature.[27] The temperature dependence of k is represented as

$$k_T = D_T = \eta_T^{-1} = \exp\left[-\frac{B'}{T - T_0}\right] \tag{10}$$

where $B' = 1200$ K and $T_0 = -100$ °C are the coefficients of the Vogel−Fulcher type for polyethylene.[28] For this reason, eq 9 predicts the same temperature dependence irrespective of the origin of the gradient field. The temperature dependence of eq 9 is then represented as

$$P(T) \propto \lambda_m(T) \propto \left(\frac{k_T}{V(T)}\right)^{1/2} \tag{11}$$

The dependence of PE- and PVDF-banded spherulites confirmed this relationship and suggested the clear experimental evidence for the instability-driven branching.[1,2] For nonbanded spherulites, instead of the relationship between the band spacing and the maximum lamellar width, it has been shown that the maximum lamellar width, λ_m, limits the persistence length of lamellar orientation along the radial direction, L, and hence similar proportional dependence of $L \propto \lambda_m \propto (k/V)^{1/2}$ is followed from eq 2. The relationship has been experimentally confirmed for the nonbanded spherulites of PB-1 in our previous work.[3]

In the previous papers,[1−3] the identification of the gradient field has yet remained to be clarified. In order to differentiate the possible origins of the gradient field, we need to examine the molecular weight dependence of the relationship. The following dependences on molecular weight will be supposed for the cases of compositional gradient and pressure gradient. First, it is supposed that the compositional gradient will be strongly dependent on the molecular weight distribution; e.g., the possibility must be ruled out for the formation of spherulites of monodispersed long paraffin.[29] Second, the M_w dependences of D and η^{-1} are known to be different as $D \propto M_w^{-2}$ and $\eta^{-1} \propto M_w^{-3.64}$,[28] depending on the respective processes of polymer chains in the reptation dynamics. Therefore, for the compositional gradient, due to the dependence of D and that of x_1 in eq 5, eq 9 suggests the molecular weight dependence of the products of P^2V and λ_m^2V represented as

$$P^2V \propto \lambda_m^2V \propto x_1D \propto f\left(\frac{M_w}{M_n}\right)M_w^{y-2} \tag{12}$$

where $f(M_w/M_n)$ represents the effect of molecular weight distribution and the power, $y > 0$, is determined by the change of the molecular weight, x_1, of the fraction rejected at the growth front for the respective M_w of the sample.

On the other hand, for the pressure gradient of eq 8, eq 9 suggests that the products of P^2V and λ_m^2V will have the power of -3.64 due to the molecular weight dependence of η

$$P^2V \propto \lambda_m^2V \propto \eta^{-1} \propto M_w^{-3.64} \tag{13}$$

It is noted that the relationship of $\eta \propto M_w^{3.64}$ also holds for a blend of polymers of the same chemical structure but different weight-averaged molecular weights,[30] in which the weight-averaged molecular weight, M_w, is by definition represented as $M_w = w_1M_{w1} + w_2M_{w2}$ with the weight fractions, w_1 and w_2, of the fractions having the weight-averaged molecular weight of M_{w1} and M_{w2}.

In the following experiments, the molecular weight dependence of P^2V and λ_m^2V is examined for the growth of the banded spherulites of PE with various M_w and M_w/M_n.

3. Experimental Section

Linear polyethylene samples with various M_w and M_w/M_n are tabulated in Table 1. The samples of 14N, 32N, 52N, and 120N were purchased from NIST (Gaithersburg, MD), and 21F, 37F, 60F,

Table 1. Molecular Characteristics of Linear PE Samples

sample	$M_w \times 10^{-3}$	M_w/M_n	sample	$M_w \times 10^{-3}$	M_w/M_n
14N	13.6	1.19	21F	20.5	1.46
32N	32.1	1.11	37F	36.5	1.30
52N	52.0	2.90	60F	60.0	1.48
120N	119.6	1.19	153F	153.0	1.72
23M	22.9	1.43	14N/32N = 1/1		
67M	66.6	3.32	14N/120N = 1/1		
76M	75.9	1.73	32N/120N = 1/1		

Table 2. Molecular Characteristics of HPBD Samples (Left) Corresponding 1:1 Blends with PE 32N (Right)

sample	$M_w \times 10^{-3}$	M_w/M_n	sample	$M_w \times 10^{-3}$	M_w/M_n
13P	13.1	1.05	23B	22.6	1.33
34P	34.3	1.04	33B	33.2	1.10
68A	68.2	1.07	50B	50.2	1.29
111P	111.5	1.08	72B	71.8	1.63

and 153F were from Fluka (Buchs, Switzerland). The samples of 23M, 67M, and 76M were obtained by mixing the fractions of 14N, 32N, and 120N in the ratio of 1:1 by weight. The ratio, M_w/M_n, of the mixture was estimated under the assumption of log-normal distribution of molecular weight in the fractions. By examining samples of different M_w and M_w/M_n, the effects of composition or viscosity in the molten state can be examined. However, since those PE are all linear and crystallizable, the change of the samples also influences the crystalline morphology due to different M_w, M_w/M_n, the degree of chain defects, etc. In order to see the effect only on the molten state of M_w and M_w/M_n, we have also examined the blend of linear PE with hydrogenated polybutadiene (HPBD), which has chemical structures similar to low-density polyethylene and very narrow molecular weight distribution, i.e., $M_w/M_n < 1.1$. Table 2 shows the details of the blends (23B, 33B, 50B, and 72B) of 32N PE and the fractions of HPBD (13P, 34P, 68A, and 111P). The HPBD samples of 13P, 34P, and 111P were purchased from Polymer Source (Dorval, Canada), and those of 68A were from American Polymer Standards (Mentor, OH). The blend ratio was 1:1 in weight. The melting temperatures of HPBD fractions were all below 110 °C and lower than the crystallization temperature examined in the present experiments. Therefore, HPBD behaves as a solvent and only influences the liquid state, while the linear PE of 32N is the only fraction to crystallize from the blends.

For the crystallization from the melt, a film of several μm thick was prepared on a cover glass by solution casting, melted at 160 °C for 2 min., crystallized isothermally at 112−118 °C. After the isothermal crystallization for a preset time interval, the sample was quenched in a freezing isopentane (∼−160 °C) by dropping the cover glass from the crystallization cell. Owing to the thin sample thickness (approximately several μm) the quench was almost instantaneous.

In order to check the effect of phase separation of linear PE and HPBD, the blend was kept at 160 °C for more than 1 h before crystallization. It was confirmed that the final morphology was not influenced by the melting time and there were no indications of phase separation for the examined range of molecular weight, as seen in the quenched portions of the AFM images of Figure 8. We have also examined the blend of 32N PE with a higher molecular weight HPBD fraction of $M_w = 289,710$ and $M_w/M_n = 1.11$. However, it seems that the blend was influenced by the miscibility, and the obtained results of the growth rate, V, and the band spacing, P, were irreproducible with the blend.

The spherulites were examined with a polarizing optical microscope (BX51, Olympus Corp.) for the measurements of the ring period and the growth rate from the change in size with crystallization time. For the microscopic examination of lamellar crystals at the growth front of spherulites, the surrounding microcrystallites and amorphous portions formed on quenching were removed by permanganic etching.[31] The samples were then examined with an atomic force microscope (SPI3800N, Seiko Instruments Inc.) in a dynamic force mode in air. Silicon cantilevers (SI-DF20, Seiko Instruments Inc.) with a resonance frequency of 110−150 kHz were used for the observations. By AFM, we have measured the lateral width of crystals at the growth front. We have determined the maximum lamellar width, λ_m, by averaging the size of several large crystals, which were placed at the growth front of different locations in spherulites. The data scatter was as much as ±30%.

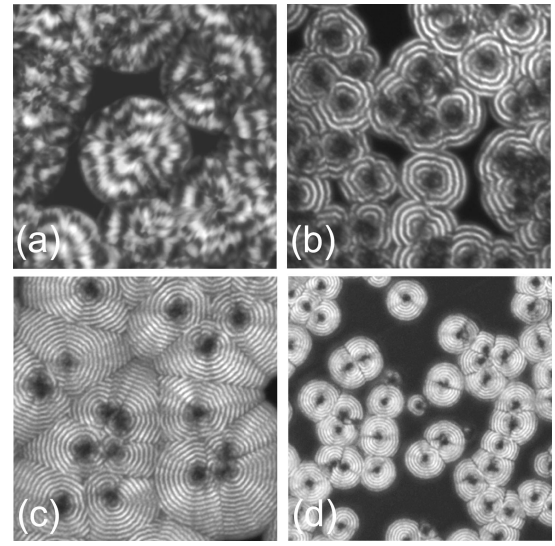

Figure 3. 100 × 100 μm^2 POM images of PE banded spherulites of (a) 14N, (b) 32N, (c) 52N, and (d) 120N, respectively, grown from the melt at 114 °C. In order to eliminate the Maltese cross of spherulites, two images of the same area differing the polarization direction by 45° are superimposed.

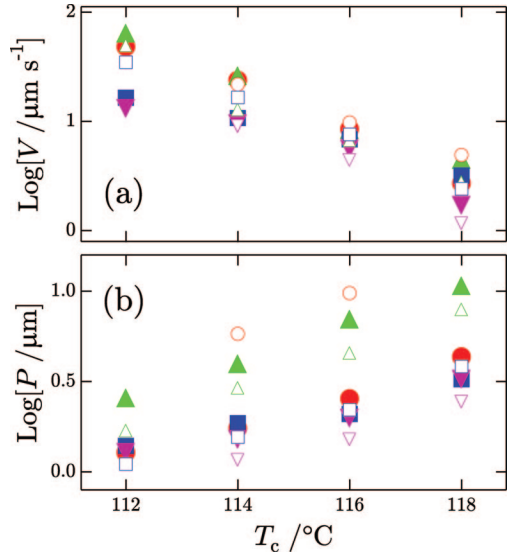

Figure 4. Logarithmic plots of (a) growth rate, V, and (b) band spacing, P, against crystallization temperature. Symbols represent the results of 21F (○), 37F (△), 60F (□), 153F (▽), 52N (●), 23 M (▲), 67 M (■), and 76 M (▼), respectively.

4. Results and Discussion

Figures 3 shows the POM images of PE spherulites of 14N, 32N, 52N, and 120N fractions at the crystallization temperature of 114 °C. It is clearly seen that the ring period undergoes consistent change with molecular weight. Similar changes have also been seen for other molecular weight samples. Figure 4 shows the growth rate, V, and the band spacing, P, plotted against crystallization temperatures for the various molecular weight samples. The data are also shown in the double logarithmic plots of P against V/k_T in Figure 5. The slope of

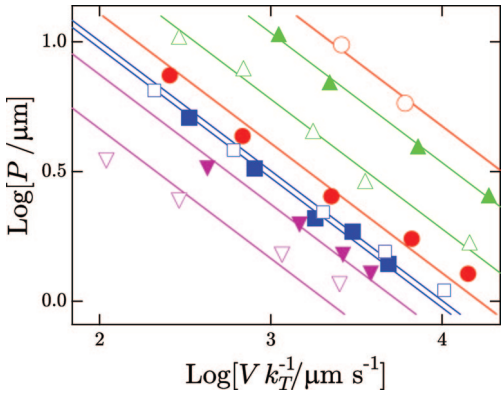

Figure 5. Double logarithmic plots of P and V shown in Figure 4. The velocity, V, is divided by k_T. Symbols represent the results of 21F (○), 37F (△), 60F (□), 153F (▽), 52N (●), 23 M (▲), 67 M (■), and 76 M (▼), respectively. The slopes of the fitting lines are all −0.5.

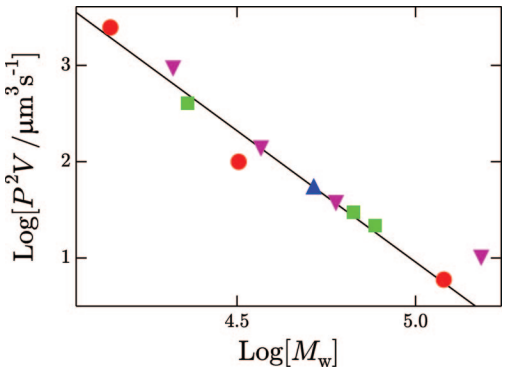

Figure 6. Double logarithmic plots of the product, P^2V, against M_w at the fixed crystallization temperature of 116 °C. Symbols represent the results of 14N, 32N, and 120N (●), 52N (▲), 21F, 37F, 60F, and 153F (▼), and 23M, 67M, and 76 M (■), respectively. The slope of the fitting line is −2.7.

the lines in Figure 5 are all −0.5 and the fitting is good enough. The results reconfirm the relationship of eq 11 reported for 32N and 120N PE fractions in our previous paper.[1]

Figure 6 shows the double logarithmic plots of the product of P^2V against the weight-averaged molecular weight, M_w, at the fixed crystallization temperature of 116 °C. In Figure 6, it is clearly seen that the data points are on a single straight line except for the highest M_w fraction of 153F. The fitting to the single line is fairly well, irrespective of the molecular weight distribution represented by M_w/M_n, which is in the range of 1.11−3.32, as shown in Table 1. It should be stressed that the mixtures of 23M, 67M, and 76 M are also on the line, in spite of the bimodal distribution of molecular weights. The insensitiveness of band spacing, P, on the molecular weight distribution has been reported by Keith and Padden[32] for a mixture of sharp fractions compared with an unfractionated PE having similar M_w and broad distribution. The present results confirmed the behavior as the plots of P^2V instead of P. On the basis of the present model associating the band spacing with the instability-driven branching, the insensitiveness suggests that the origin of the instability cannot be the compositional gradient originally proposed by Keith and Padden.[13] This conclusion on the PE samples with various molecular weight distributions is in accordance with the result of monodispersed long paraffin evolving banded and nonbanded spherulites;[29] the formation of spherulites with the monodispersed long paraffin obviously excluded the possibility of compositional gradient as the origin of instability-driven branching for that system.

On the other hand, the slope of the straight fitting line (excluding the highest M_w fraction of 153F) in Figure 6 was −2.7. The absolute value of the slope is larger than the power expected for the compositional gradient, eq 12, but smaller than that for the pressure gradient, eq 13. In the previous paper, the molecular weight dependence of the maximum lamellar width has also been examined for 14N, 32N and 120N fractions. The results indicated the dependence of λ_m^2V proportional to $M_w^{-1.8}$, which was also weaker than the power for the pressure gradient. As has been mentioned in the Experimental Section, those examined PE samples are all linear and crystallizable, so that the different samples can have different crystalline morphologies and the folding regions as well as the molten states, depending on M_w, M_w/M_n, the degree of chain defects, etc. The obtained power as well as the deviation of the highest molecular weight fraction of 153F can therefore have the influence of the different crystalline morphologies and the folding regions. The difference between the power of P (−2.7) and λ_m (−1.8) can also be explained as the influence on the coefficient, $g/\Delta\theta$, in eq 1; namely, the difference can be explained by the dependence of $g/\Delta\theta \propto M_w^{-0.9}$, which is probable due to larger $\Delta\theta$ with more congestion in the folding regions for higher molecular weight, as has been noted in our previous paper,[1] and due to smaller axial ratio of growth rate, g, for higher molecular weight, which has been confirmed for isolated single crystals in the bulk melt.[33] We have assumed the ratio in spherulites will not be far from that of isolated lamella. It is noted that the lamellar crystals in spherulites are confined by surrounding lamellar crystals so that the growth in width may be different from the growth in isolated lamellar crystals; i.e., the growth can be influenced by the confinement and may be nonlinear. The manner of lamellar twist in spherulites may also be affected by the confinement.

In order to remove the effects on the coefficient, $g/\Delta\theta$, in eq 1 of crystallization temperature, of molecular weight, and of the resultant changes in the confinement and in nonplanar morphology of lamellae, and to see the effect of M_w only on the molten state, we have examined the blend of linear PE with hydrogenated polybutadiene (HPBD), having melting temperatures well below the examined crystallization temperatures with negligible influence of phase separation in the examined ranges of temperature, molecular weight, and time. By doing the examination, the crystallizing part was fixed to that of linear PE so that the coefficient, $g/\Delta\theta$, was supposed to be fixed at the fixed composition and temperature. Since the effect of confinement is fixed and our modeling does not assume any specific mechanism of lamellar twisting, we think the analysis can be applicable even for possible nonlinear growth along the width with lamellar twisting under the confinement in spherulitic growth.

Figure 7 shows the POM images of PE spherulites from the 1:1 blends of PE 32N and HPBD fractions of different M_w at the fixed crystallization temperature of 116 °C. Figure 8 shows the AFM images of the lamellar crystals at the growth fronts of those spherulites. It is again clearly seen that both of the band spacing and the lateral width of crystals undergo consistent changes with the weight-averaged molecular weight, M_w.

Figure 9 shows the growth rate, V, and the band spacing, P, plotted against crystallization temperatures for the blends. The data are also shown in the double logarithmic plots of P against V/k_T in Figure 10 confirming the reasonable fitting with the straight lines of the slope, −0.5, expected from the relationship of eq 11. Figure 11 shows the double logarithmic plots of the products of P^2V and λ_m^2V against the weight-averaged molecular weight, M_w, at 116 °C. The data points of P^2V and λ_m^2V are on straight lines having the slopes of −3.9 and −3.6, respectively. For the blends, both values are close to the power expected for the M_w dependence of the viscosity, −3.64, as shown in eq 13. Therefore, we have successfully confirmed the prediction of eq 13 suggesting the instability of growth front caused by the

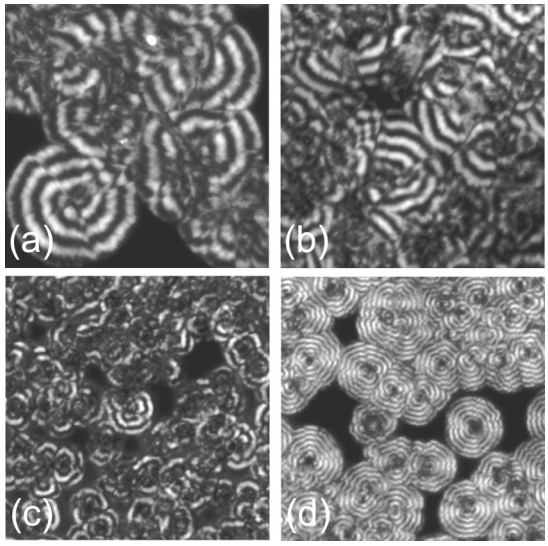

Figure 7. 100 × 100 μm^2 POM images of PE banded spherulites of (a) 23B, (b) 33B, (c) 50B, and (d) 72B blends, respectively, grown from the melt at 116 °C. In order to eliminate the Maltese cross of spherulites, two images of the same area differing the polarization direction by 45° are superimposed.

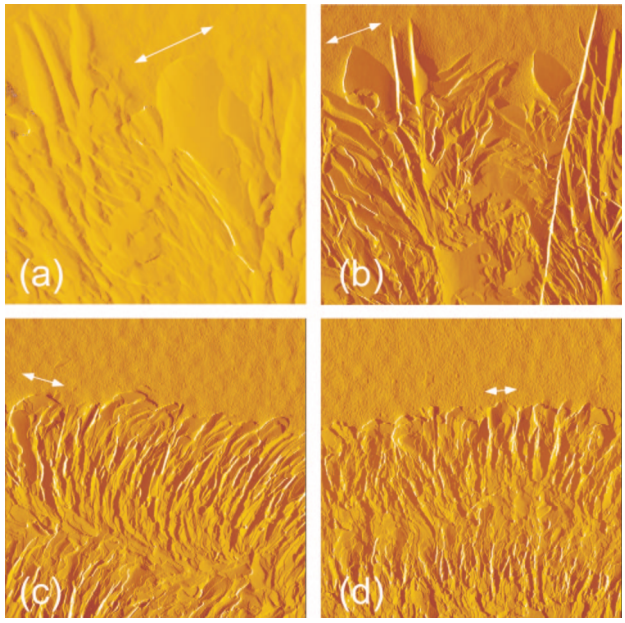

Figure 8. 5 × 5 μm^2 AFM amplitude images near the growth front of polyethylene spherulites of (a) 23B, (b) 33B, (c) 50B, and (d) 72B blends, respectively, grown from the melt at 116 °C.

pressure gradient due to the difference in the crystalline and molten densities.

For the pressure gradient, the thickness of the shear flow can be estimated from the experimental data by using eq 8, as follows:

$$b = \lambda_m \left[2\pi \frac{v_s}{\Delta v} \left(\frac{\gamma}{12\eta V} \right)^{1/2} \right]^{-1} \tag{14}$$

where v_s and Δv are expressed as

$$v_s = \frac{1}{\rho_c} \frac{M_{seg}}{N_A} \tag{15}$$

$$\Delta v = \left(\frac{1}{\rho_m} - \frac{1}{\rho_c} \right) \frac{M_{seg}}{N_A} \tag{16}$$

with the densities of crystalline and molten states, $\rho_c = 0.97$ g/cm^3 [34] and $\rho_m = 0.8$ g/cm^3,[35] respectively, the molecular

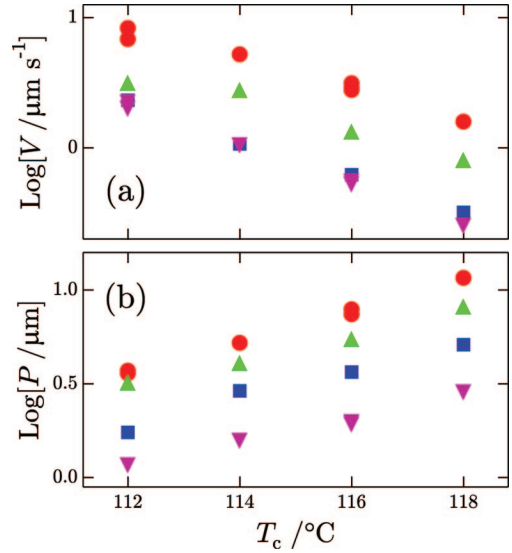

Figure 9. Logarithmic plots of (a) growth rate, V, and (b) band spacing, P, against crystallization temperature. Symbols represent the results of 23B (●), 33B (▲), 50B (■), and 72B (▼) blends, respectively.

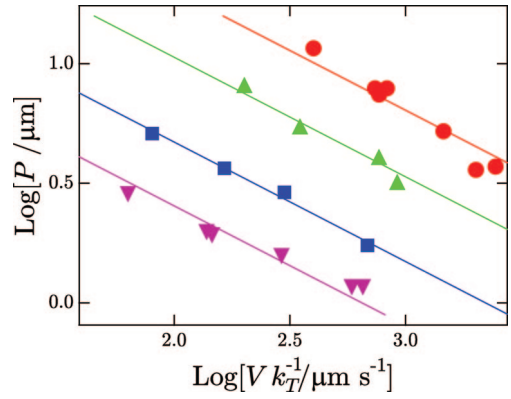

Figure 10. Double logarithmic plots of P and V shown in Figure 9. The velocity, V, is divided by k_T. Symbols represent the results of 23B (●), 33B (▲), 50B (■), and 72B (▼) blends, respectively. The slopes of the fitting lines are all −0.5.

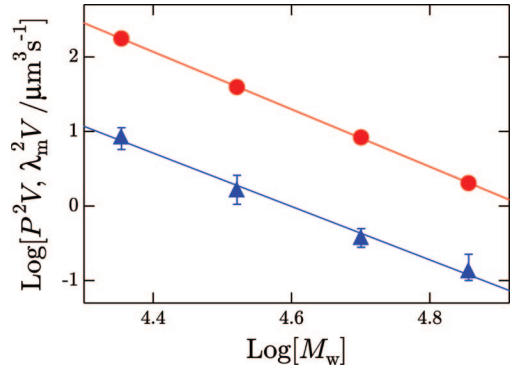

Figure 11. Double logarithmic plots of the product, P^2V (●) and $\lambda_m^2 V$, (▲) against M_w for the 23B, 33B, 50B, and 72B blends at the fixed crystallization temperature of 116 °C. The slopes of the fitting lines are −3.9 and −3.6 for P^2V and $\lambda_m^2 V$, respectively.

weight of the segment, M_{seg}, and the Avogadro number, N_A. The surface tension, γ, in eq 14 is roughly estimated to be 10 erg/cm [2,36] and the viscosity is estimated as $\eta = 10^{-13} M_w^{3.64}$ P at 118 °C from the literature data[28] by using eq 10. The obtained results for the data in Figure 11 are shown in the plots against M_w in Figure 12a. It is seen that the thickness of shear flow

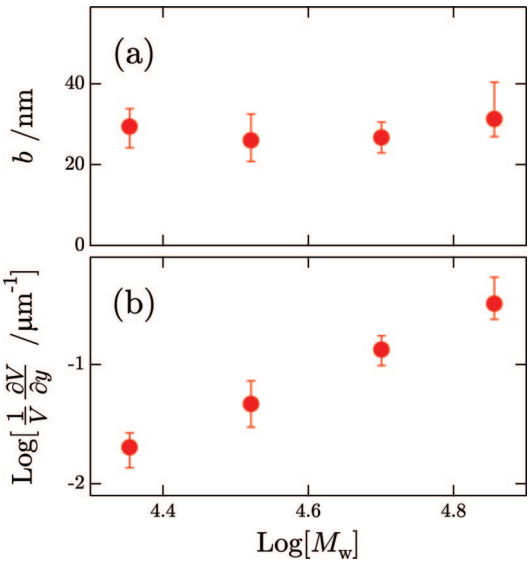

Figure 12. Plots of (a) the thickness of shear flow, b, and (b) the relative ratio of the gradient of growth rate, $(1/V)(\partial V/\partial y)$, against M_w for the 23B, 33B, 50B, and 72B blends determined from the data shown in Figures 9 and 11.

remains almost constant for the molecular weight examined in the present experiments. It seems that the thickness of about 30 nm corresponds to single lamella or the bundle of a few lamellar crystals.

For the instability driven by the pressure gradient, it will also be meaningful to estimate the gradient of growth rate as the result of the gradient of supercooling ahead of the growth front. The gradients are related as follows:

$$\frac{1}{V}\frac{\partial V}{\partial y} = \frac{\mathrm{d}\log V}{\mathrm{d}T}\frac{\partial(\Delta T)}{\partial y} \tag{17}$$

and the gradient of supercooling is determined by the pressure gradient from the relationship of eq 6, as follows:

$$\frac{\partial(\Delta T)}{\partial y} = T_m\frac{\Delta v}{\Delta h_f}\frac{\partial p}{\partial y} \tag{18}$$

where $T_m \simeq 140$ °C[36] and the heat of fusion per segment, Δh_f, is expressed by that per unit volume, $\Delta h_f^{vol} \simeq 2.8 \times 10^9$ erg/cm^3,[36] as

$$\Delta h_f = \frac{\Delta h_f^{vol}}{\rho_c}\frac{M_{seg}}{N_A} \tag{19}$$

The pressure gradient in eq 18 can be estimated experimentally from the lamellar width, λ_m, by using eqs 4 and 6, as follows:

$$\frac{\partial p}{\partial y} = \left(\frac{2\pi}{\lambda_m}\right)^2\frac{v_s}{\Delta v}\gamma \tag{20}$$

From eqs 15−20, the relative ratio of the gradient of growth rate is obtained as

$$\frac{1}{V}\frac{\partial V}{\partial y} = \frac{\gamma T_m}{\Delta h_f^{vol}}\frac{\mathrm{d}\log V}{\mathrm{d}T}\left(\frac{2\pi}{\lambda_m}\right)^2 \tag{21}$$

Figure 12b shows the relative ratio of the gradient of growth rate estimated from the experimental results of d log V/dT and λ_m shown in Figures 9 and 11, respectively. The ratio showed strong dependence on molecular weight (viscosity) and changes from 2 up to 32%/μm. The ratio is noticeable and can be the cause of the fluctuations in the growth rate of individual lamellar crystals at the growth front of spherulites; the fluctuations have been actually reported by in situ AFM observations of the growth front of polymer spherulites.[37,38]

5. Conclusion

We have examined the formation mechanism of polymer spherulites with chain-folded lamellar crystallites filling the three-dimensional space by way of consecutive branching and reorientation. In our previous papers,[1−3] we have considered a branching mechanism due to growth-front instability, the possibility of which has been discussed for many years without successful experimental confirmations. Our modeling was based on the instability-driven branching and the reorientation of lamellar crystals due to the inherent stresses on the folding surfaces. The modeling has common features with the morphological observations of the repetitive lamellar twisting and splaying in a banded spherulite of PVDF confirmed by Briber and Khoury[14] and the branching and splaying of individual dominant lamellae confirmed by Bassett et al. for the spherulites of polyethylene,[15] isotactic polypropylene,[16] and isotactic polystyrene.[17] In the previous papers, we have experimentally confirmed the predicted relationship between the growth rate, the lamellar width at the growth front, and the band spacing of banded spherulites of polyethylene[1] and PVDF[2] or the persistence length of nonbanded spherulites of poly(butene-1)[3] by examining the temperature dependences. In the present paper, as the continuing work on the mechanism of instability-driven branching, the origin of the instability has been approached by the examination of the dependences on the average and distribution of molecular weights.

As the origins of the instability, the possibilities have been suggested for the compositional gradient of essentially multicomponent system of synthetic polymers and for the pressure gradient due to the density difference between the crystal and the melt. By examining the temperature dependences, due to the same dependences of the diffusion coefficient and the inverse of viscosity, the distinction of the predicted dependences could not be made in the previous papers. By the examination of the dependences on the average and distribution of molecular weights, the differentiation of the mechanisms can be made because of the expected strong dependence of the effect of compositional gradient on the distribution and of the different dependences of the diffusion coefficient and the inverse of viscosity on the weight-averaged molecular weight, M_w.

Experimentally, several molecular weight fractions of linear PE, unfractionated linear PE, and the mixtures of the fractions have been examined in terms of the band spacing and the growth rate. The obtained results showed the insensitivity to the molecular weight distribution, and hence excluded the possibility of compositional gradient as the origin of the instability. On the other hand, the quantitative examination of the M_w dependence indicated a dependence weaker than predicted for the pressure gradient. It has been supposed that the linear PE samples with different M_w, M_w/M_n, chain defects, etc. may have influence on the crystal morphology and folding regions as well as on the viscosity of the melt. Then, in order to examine the effect of molecular weight only on the viscosity, a fraction of linear PE was blended with HPBD fractions which stay in the molten state in the examined temperatures. The results of the dependences of band spacing and lamellar width on the weight-averaged molecular weight followed the dependence of viscosity and supported the prediction of the instability due to pressure gradient. From those results of the dependences on the weight-averaged molecular weight and the insensitivity to the distribution of molecular weights, it is concluded that the origin of the instability in polyethylene banded spherulites is the pressure gradient ahead of the growth front.

It should be noted that the relationships confirmed in the present results can be expected for both of the cases of

nonuniform reorientation on the occasion of branching and continuous reorientation limited by lamellar width. So, by the present experimental results, we do not intend to suggest either of the two possible cases. Actually, there have been prior studies suggesting both of the continuous twist of individual polymer crystals[38−43] and the nonuniform twisting amplified on branching.[15,38] On the other hand, the lateral growth habit of crystals with sectorization having different stem tilts and subcell distortions will also have an influence on the nonplanar conformation of lamellar crystals. The manner and the role of nonplanar conformation of lamellar crystals in spherulites are important issues but are beyond the scope of the present phenomenological approach. Those will be the issues to be clarified in future works. The important point in the present results is the confirmation of the role of pressure gradient in the instability-driven branching of lamellar crystals in polyethylene banded spherulites. The instability-driven branching has also been concluded for nonbanded spherulites of poly(butene-1),[3] so that the branching is not the determining factor for the formation of banded spherulites. Instead, we think the mechanism of instability-driven branching will be an important factor in the structural formation of polymer spherulites in general.

For the generalization of the present conclusion of polyethylene-banded spherulites, it is important to be justified by further examinations with other polymer systems including nonbanded spherulites. It is also noted that the temperature dependence of the diffusion coefficient is known to decouple from that of viscosity near the glass transition temperature.[27] A recent proposal on the formation mechanism of spherulites is based on the decoupling.[44,45] It will be possible to utilize the decoupling of the temperature dependence for the further examination of the origin of instability-driven branching.

Acknowledgment. The authors thank Prof. S. Tanaka of Hiroshima University, Prof. Y. Yamazaki of Waseda University, and Prof. T. Taniguchi of Yamagata University for helpful discussions. This work was partially supported by MEXT Japan, Grant-in-Aid for Scientific Research on Priority Areas, "Creation of Nonequilibrium Soft Matter Physics".

References and Notes

(1) Toda, A.; Okamura, M.; Taguchi, K.; Hikosaka, M.; Kajioka, H. *Macromolecules* **2008**, *41*, 2484.
(2) Toda, A.; Taguchi, K.; Hikosaka, M.; Kajioka, H. *Polym. J.* **2008**, in press (DOI: 10.1295/polymj.PJ2007191).
(3) Kajioka, H.; Hikosaka, M.; Taguchi, K.; Toda, A. *Polymer* **2008**, *49*, 1685.
(4) Point, J. J. *Bull. Acad. R. Belg.* **1953**, *41*, 982.
(5) Keith, H. D.; Padden, F. J., Jr. *J. Polym. Sci.* **1959**, *39*, 123.
(6) Price, F. P. *J. Polym. Sci.* **1959**, *39*, 139.
(7) Keller, A. *J. Polym. Sci.* **1959**, *39*, 151.
(8) Fujiwara, Y. *J. Appl. Polym. Sci.* **1960**, *4*, 10.
(9) Nozue, Y.; Hirano, S.; Kurita, R.; Kawasaki, N.; Ueno, S.; Iida, A.; Nishi, T.; Amemiya, Y. *Polymer* **2004**, *45*, 8299.
(10) Kajioka, H.; Yoshimoto, S.; Gosh, R. C.; Tanaka, S.; Taguchi, K.; Toda, A. Manuscript in preparation.
(11) Lotz, B.; Cheng, S. Z. D. *Polymer* **2005**, *46*, 577.
(12) Bassett, D. C. *J. Macromol. Sci.* **2003**, *B42*, 227.
(13) Keith, H. D.; Padden, F. J., Jr. *J. Appl. Phys.* **1963**, *34*, 2409.
(14) Briber, R. M.; Khoury, F. *J. Polym. Sci. B: Polym. Phys.* **1993**, *31*, 1253.
(15) Bassett, D. C.; Hodge, A. M. *Proc. R. Soc.* **1981**, *A377*, 61.
(16) Bassett, D. C.; Olley, R. H. *Polymer* **1984**, *25*, 935.
(17) Bassett, D. C.; Vaughan, A. S. *Polymer* **1985**, *26*, 717.
(18) Frank, F. C. *Discuss. Faraday Soc.* **1979**, *68*, 7.
(19) Muthukumar, M. Presented at the 234th ACS National Meeting, Boston, Aug. 19−23, 2007; Paper no. PMSE 455.
(20) Mullins, W. W.; Sekerka, R. F. *J. Appl. Phys.* **1963**, *34*, 323; **1964**, *35*, 444.
(21) Langer, J. S. *Rev. Mod. Phys.* **1980**, *52*, 1.
(22) Flory, P. J. *Principles of Polymer Chemistry*; Cornell University Press: Ithaca, NY, 1953; Chapter 12.
(23) Goldenfeld, N. *J. Cryst. Growth* **1987**, *84*, 601.
(24) Schultz, J. M. *Polymer Crystallization*; Oxford University Press: Oxford, UK, 2001; Chapter 10.
(25) Saffman, P. G.; Taylor, G. I. *Proc. R. Soc. Ser. A* **1958**, *245*, 312.
(26) Fields, R. J.; Ashby, M. F. *Philos. Mag.* **1976**, *33*, 33.
(27) Ngai, K. L.; Magill, J. H.; Plazek, D. J. *J. Chem. Phys.* **2000**, *112*, 1887.
(28) Pearson, D. S.; Ver Strate, G.; von Meerwall, E.; Schilling, F. C. *Macromolecules* **1987**, *20*, 1133.
(29) Bassett, D. C.; Olley, R. H.; Sutton, S. J.; Vaughan, A. S. *Macromolecules* **1996**, *29*, 1852.
(30) Friedman, E. M.; Porter, R. S. *Trans. Soc. Rheol.* **1975**, *19*, 493.
(31) Olley, R. H.; Hodge, A. M.; Bassett, D. C. *J. Polym. Sci., Polym. Phys.* **1979**, *17*, 627.
(32) Keith, H. D.; Padden, F. J., Jr. *Macromolecules* **1996**, *25*, 7776.
(33) Toda, A.; Okamura, M.; Hikosaka, M.; Nakagawa, Y. *Polymer* **2005**, *46*, 8708.
(34) Cole, E. A.; Holmes, D. R. *J. Polym. Sci.* **1960**, *46*, 245.
(35) Orwoll, R. A.; Flory, P. J. *J. Am. Chem. Soc.* **1967**, *89*, 6814.
(36) Hoffman, J. D.; Davis, G. T.; Lauritzen, J. I., Jr. *Treatise on Solid State Chemistry*; Plenum Press: New York, 1976; Vol. *3*, Chapter 7.
(37) Hobbs, J. K.; Humphris, A. D. L.; Miles, M. J. *Macromolecules* **2001**, *34*, 5508.
(38) Xu, J.; Guo, B.-H.; Zhang, Z.-M.; Zhou, J.-J.; Jiang, Y.; Yan, S.; Li, L.; Wu, Q.; Chen, G.-Q.; Schultz, J. M. *Macromolecules* **2004**, *37*, 4118.
(39) Keller, A.; Sawada, S. *Makromol. Chem.* **1964**, *74*, 190.
(40) Kunz, M.; Dreschler, M.; Möller, S. *Polymer* **1995**, *36*, 1331.
(41) Lotz, B.; Gonthier-Vassal, A.; Brack, A.; Magoshi, J. *J. Mol. Biol.* **1982**, *156*, 345.
(42) Li, C. Y.; Yan, D.; Cheng, S. Z. D.; Bai, F.; He, T.; Chien, L.-C.; Harris, F. W.; Lotz, B. *Macromolecules* **1999**, *32*, 524.
(43) Li, C. Y.; Cheng, S. Z. D.; Weng, X.; Ge, J. J.; Bai, F.; Zhang, J. Z.; Calhoun, B. H.; Harris, F. W.; Chien, L.-C.; Lotz, B. *J. Am. Chem. Soc.* **2001**, *123*, 2462.
(44) Gránásy, L.; Pusztai, T.; Börzsönyi, T.; Warren, J. A.; Douglas, J. F. *Nat. Mater.* **2004**, *3*, 645.
(45) Gránásy, L.; Pusztai, T.; Tegze, G.; Warren, J. A.; Douglas, J. F. *Phys Rev. E* **2005**, *72*, 011605.

MA800994G